Beyond the ensemble average: X-ray microdiffraction analysis of single SiGe islands

C. Mocuta,[1] J. Stangl,[2] K. Mundboth,[1,2] T. H. Metzger,[1] G. Bauer,[2] I. A. Vartanyants,[3] M. Schmidbauer,[4] and T. Boeck[4]

[1]*European Synchrotron Radiation Facility (ESRF), B.P. 220, F-38043 Grenoble Cedex, France*
[2]*Institut für Halbleiter- und Festkörperphysik, Johannes Kepler Universität Linz, AltenbergerstraBe 69, A-4040 Linz, Austria*
[3]*Hasylab at DESY, Notkestr. 85, D-22607 Hamburg, Germany*
[4]*Institute for Crystal Growth, Max-Born-StraBe 2, D-12489 Berlin, Germany*
(Received 16 April 2008; published 18 June 2008)

X-ray microdiffraction is used to analyze strain and composition profiles in individual micron-sized SiGe islands grown by liquid phase epitaxy on Si(001) substrates. From the variation of the scattered intensity while scanning the sample through a focused x-ray beam of few μm size, an image of the island distribution on the sample is created. Using this image it is possible to identify particular islands and select them for analysis one by one. The Ge and strain distribution within each island is obtained from the intensity distribution in reciprocal space measured for several individual islands. The detailed shape of each measured island is obtained from scanning electron microscopy. Apart from truncated pyramid-shaped islands, we detect and characterize a small number of flat islands and show that they represent an earlier growth stage of the pyramidal shaped ones. This analysis is only possible by combining the local x-ray diffraction with scanning electron microscopy on exactly the same islands.

I. INTRODUCTION

Chemical composition and strain distribution are two key parameters determining many structural and electronic properties of semiconductor micro- and nanostructures. With the development of small structures for electronics and photonics, the use of local probes is becoming more and more common to obtain information at short length scales and thus an understanding of properties related to the small size. In order to achieve local/spatial resolution, well-established transmission electron microscopy or scanning-probe methods are routinely used, but these methods are limited to investigations of surfaces, thinned, or cleaved samples.[1,2] Due to the rather complex and often destructive sample preparation required for these methods, they do not provide straight forward means to isolate a *particular* micro- or nanometer-sized object for analysis. X-ray diffraction (XRD) is the method of choice to analyze structural parameters nondestructively. In the case of semiconductor islands deposited by self-assembled growth, the strain fields and spatial distributions of the constituting elements have been determined with resolutions down to the nanometer range (for reviews see, e.g., Refs. 3 and 4). In crystalline materials, the value of the strain is directly accessible from the measurement of the unit cell dimensions and their distortions. The composition can be assessed by exploiting the variation of unit cell size as a function of composition.[5,6] Compositional refinement is provided by probing changes of the scattering power in the vicinity of fundamental absorption edges (anomalous scattering).[7–9] However, all such studies rely on the assumption of a small dispersion in the properties of many individual islands: in a conventional XRD experiment, an x-ray spot is used, which is much larger than the islands and their spatial separation. The corresponding results thus represent *ensemble averages*. So far, no XRD study permitted a measurement of an individual island combined with another local probe method on *exactly the same island*.

Hard x-ray focusing, with focal sizes in the sub-100-nm range has recently been demonstrated at several synchrotron sources.[10–12] Microbeam experiments using diffraction or small-angle scattering signals as probe have been reported.[13–17] In addition, the coherence properties of synchrotron x-ray beams have been used for imaging[18] and the three-dimensional shape and strain reconstructions of isolated nanostructures.[19,20] However, no site selectivity within an ensemble has been reported so far.

In this paper we present an approach which uses diffraction of highly focused x-ray beams to locally resolve strain and composition distributions in epitaxial micro- and nanostructured materials: we study the Ge and strain distribution in single SiGe islands grown by liquid phase epitaxy (LPE).

II. EXPERIMENTAL

The principle of our investigations on individual SiGe islands is described in Fig. 1: the x-ray beam is focused by lenses onto a small spot on the sample from where elastically scattered x-rays are detected (a). The intensity distribution around different reciprocal lattice point (RLP) positions can then be probed (b),(c). If the focused beam is scattered from the bare sample surface, the intensity distribution shows a sharp peak from the Si substrate (b), and a streak perpendicular to the sample surface, the crystal truncation rod (CTR),[21] is observed. If the x-ray beam hits an island, additional and much broader features appear in reciprocal space due to the inhomogeneous strain field and the finite size of the island (c). While measuring at a position in reciprocal space where scattering from islands is expected, the sample's lateral position is scanned in two dimensions, and the intensity is recorded as a function of the real space position. This yields an image of the island distribution on the sample (d). The local strain is responsible for the observed scattered x-ray intensity contrast. Hence the setup works similar to a scanning probe microscope, with a tunable probe signal. It is nondestructive,
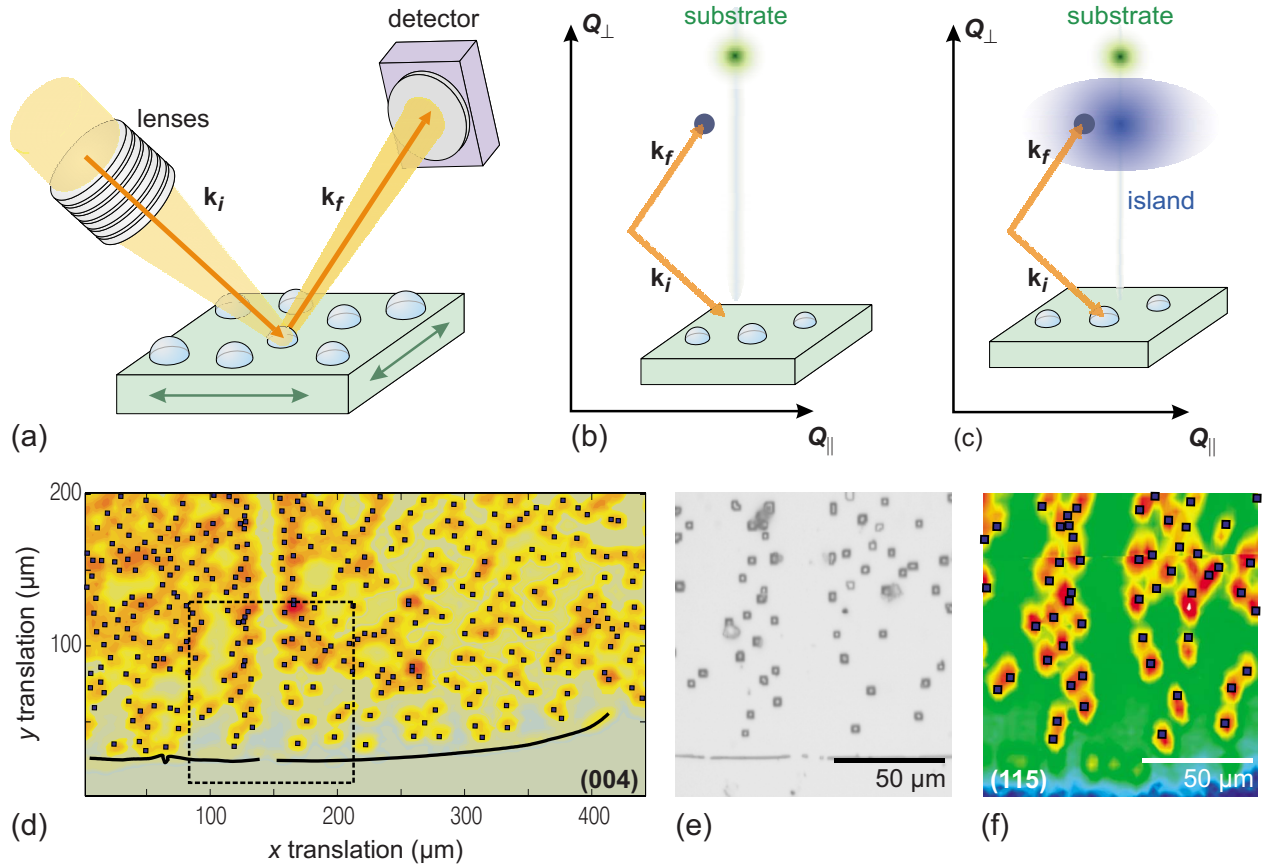
FIG. 1. (Color online) (a) Illustration of method: elastic scattering from the spot illuminated by a focused x-ray beam is detected ($\mathbf{k}_i$ and $\mathbf{k}_f$ are the scattering vectors). The x-ray spot illuminates either the area in-between islands (b) or a single island (c). Only in the latter case, a broad x-ray diffraction signal (due to lattice spacing distribution inside the SiGe islands) is observed. Tuning in reciprocal space to a position characteristic for the island [blue dot in (b), (c)] and scanning the sample laterally, higher intensity is observed whenever an island is illuminated by the x-ray spot, leading to an image of the island distribution (d). Overlaid to it are the island positions (squares) extracted from an optical microscopy image (e). (f) Similar to (d), with the local probe tuned in the vicinity of the (115) reciprocal lattice point.

sensitive both to surface and buried structures, and requires no sample preparation. This method allows the identification and analysis of particular islands one by one, which is critical for the complete characterization of the *very same* specific island by combining the x-ray results with other local-probe techniques.

In contrast to x-ray microscopy studies of grain distribution in polycrystalline samples,[22,23] where the distinction of individual grains is based on orientation differences and the spatial resolution of charge coupled device (CCD) detectors, we study epitaxially grown SiGe islands on a *single crystalline* Si substrate. Hence all islands have exactly the same orientation, and spatial distinction is obtained by illuminating only one island at a time. Due to the beam divergence introduced by the focusing, in our study the detector resolution of about 100 μm/pixel does not provide resolution in real space, but rather resolution in *reciprocal space*, which is used to determine the strain profile within a single island.

A. Samples

We apply the method to study SiGe islands grown self-organized by LPE on Si(001) substrates at a temperature of 600 °C. The island sizes are in the range of micrometers for Ge contents around 5%–10%, and go down to 30 nm for Ge contents of 85%. They are square-based truncated pyramids, with {111} side facets and a {001} top facet (see Refs. 21 and 24 for description of growth and morphology). In self-organized systems properties vary from island to island and on the nanometer scale, within the same island. It is therefore challenging to disentangle the properties of an "average" island from the variations from one island to another. This local structure determination of an individual island is, however, necessary to better characterize and understand the interplay between growth conditions and structural, optical, and electronic properties.[25] We thus analyzed islands one by one to shed more light on this subject.

B. Diffraction experiments

At beamline ID01 (ESRF, Grenoble) we employ beryllium compound refractive lenses to focus the x-ray beam and record diffraction patterns of single SiGe islands grown on Si(001). At a focus size of ~3×5 μm^2, several 10^{10} photons/second are concentrated in the focal spot, corresponding to a gain of the flux density of ~1500 compared

to the unfocused beam.[26] This gain compensates for the much lower scattering volume (one island) as compared to ensemble averaging experiments ($\sim 10^3$ islands). The reduced spot size results also in a smaller background originating from the illuminated volume surrounding the islands. To obtain a precise analysis of a single island, it has to be ensured that for all angular positions, the entire island volume scatters, i.e., the focusing, has to be well adapted to the size of the islands to be analyzed. In the present case the spot size matches very well the size of the investigated SiGe islands (base size of 3.2 μm and height of 1 μm) and is smaller than the average distance between them (up to 10 μm).

The distribution of islands can be seen in Fig. 1(d), where the lattice strain due to the variation of composition and relaxation in the SiGe islands yields the intensity contrast. Generally, in order to obtain an image of the sample, the only requirement is that different spots on a sample produce sufficiently different scattering patterns in reciprocal space. Thus, by keeping the reciprocal space position fixed, an intensity modulation is observed while translating the sample in real space.[27] As previously shown for ensembles,[28] also buried islands produce enough distinct scattering patterns to be analyzed by the presented method.

In our case the instrument was tuned to an island-sensitive position close to the (004) Bragg reflection in reciprocal space as sketched in Figs. 1(b) and 1(c), and the real space position (sample translation) was scanned. In this "scanning x-ray diffraction" (SXD) image, the high intensities (orange and red colors) represent island positions, whereas low intensities (yellow to blue colors) represent the areas in between islands. Overlaid to the SXD images are the positions of islands observed on the same area by an optical microscope [a part of which is shown in panel (e)], showing an excellent match. From this image, it is now possible to identify particular islands, and it is straight forward to select and investigate one specific island, corresponding to the spectroscopy mode of a scanning probe microscope. For each island, the intensity distribution in reciprocal space close to several Bragg points is measured [two-dimensional reciprocal space maps (RSM)]. Rotating the goniometer from one Bragg peak to another may result in the movement of an island out of the x-ray spot: since the axes of rotation of all stages do not intersect exactly at a point, but rather within the "sphere of confusion" of typically 20 μm diameter, a remapping of the same region is used to identify the same island for each Bragg peak. Figure 1(f) shows a SXD image of the area indicated in panel (d), taken in the vicinity of the (115) Bragg peak. The two maps allow us to identify, in both reflections, the same sample area and select the *very same island* for detailed structural analysis.

Figure 2 shows RSMs for the two single islands indicated in the SXD inset, as well as using an unfocused beam for comparison to the ensemble average. As the intensity of the Si substrate peak saturates the linear detector, this area was excluded from the measurements ("detector streak"), and measured separately with an attenuator in the beam. Figures 2(a) and 2(b) show RSMs taken around symmetric (004) and asymmetric (115) Bragg peaks using a conventional setup with a 300×300 μm^2 large beam, representing the statistical average over about 10^3 islands. The intensity from the
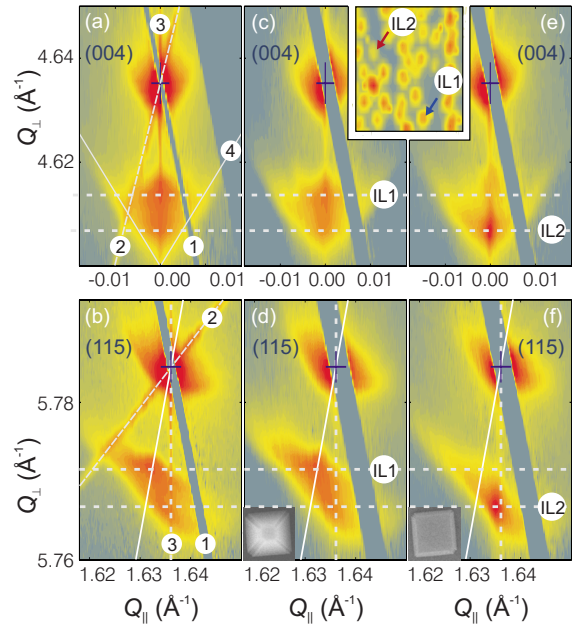

FIG. 2. (Color online) RSM of SiGe islands around (004) and (115) RLPs (log-scale intensity): (a), (b) ensemble average result over $\sim 10^3$ islands. Apart from Si substrate Bragg peak (cross) and the intensity distribution caused by the islands [cf. Figs. 1(b) and 1(c)], we identify: (1) the linear detector saturation streak, (2) the monochromator streak, (3) the Si surface CTR, and (4) facet streaks originating from the {111} island side facets. RSM from particular single islands: (c), (d) truncated pyramid-shaped islands (blue arrow in inset), and (e), (f) flat islands (red arrow in inset), respectively. The inset shows a SXD map with the measured single islands indicated by arrows; results shown in (c–f) are for the particular islands labeled IL1 and IL2 (SEM images in insets). On panels (b) (d), (f), the continuous lines represent the relaxation lines. Scattered intensity on this line is the signature of complete relaxation in the islands, while intensity along the CTR (vertical dotted line) represents pseudomorphically strained material.

islands shows extended streaks perpendicular to the {111} side facets. The maximum of the intensity (labeled "IL1") in the (115) map lies close to the relaxation line, i.e., the line linking the substrate peak with the origin of reciprocal space. Peaks lying on this line correspond to material with different lattice parameters, but the same lattice symmetry as the substrate, indicating complete relaxation of the islands. Figures 2(c) and 2(d) show the same maps recorded with the focused beam on one particular single island (IL1 in the inset). The features are almost identical to the ensemble averaged measurements, indicating that the selected island is representative of the island majority. Figures 2(e) and 2(f) show RSMs recorded from another island in the x-ray spot (IL2 in the inset). Here the intensity distribution is rather different: the maximum "IL2" is shifted in the (115) map to a position directly beneath the substrate peak, i.e., the in-plane lattice spacing of the island is almost the same as the substrate's, thus the island is pseudomorphically strained with respect to the Si substrate. Due to the elastic response of the island, the lattice spacing perpendicular to the surface is larger than for the "average" island, and the peak appears at a lower value of $Q_\perp$ in both the (004) and (115) maps. From mere inspec-
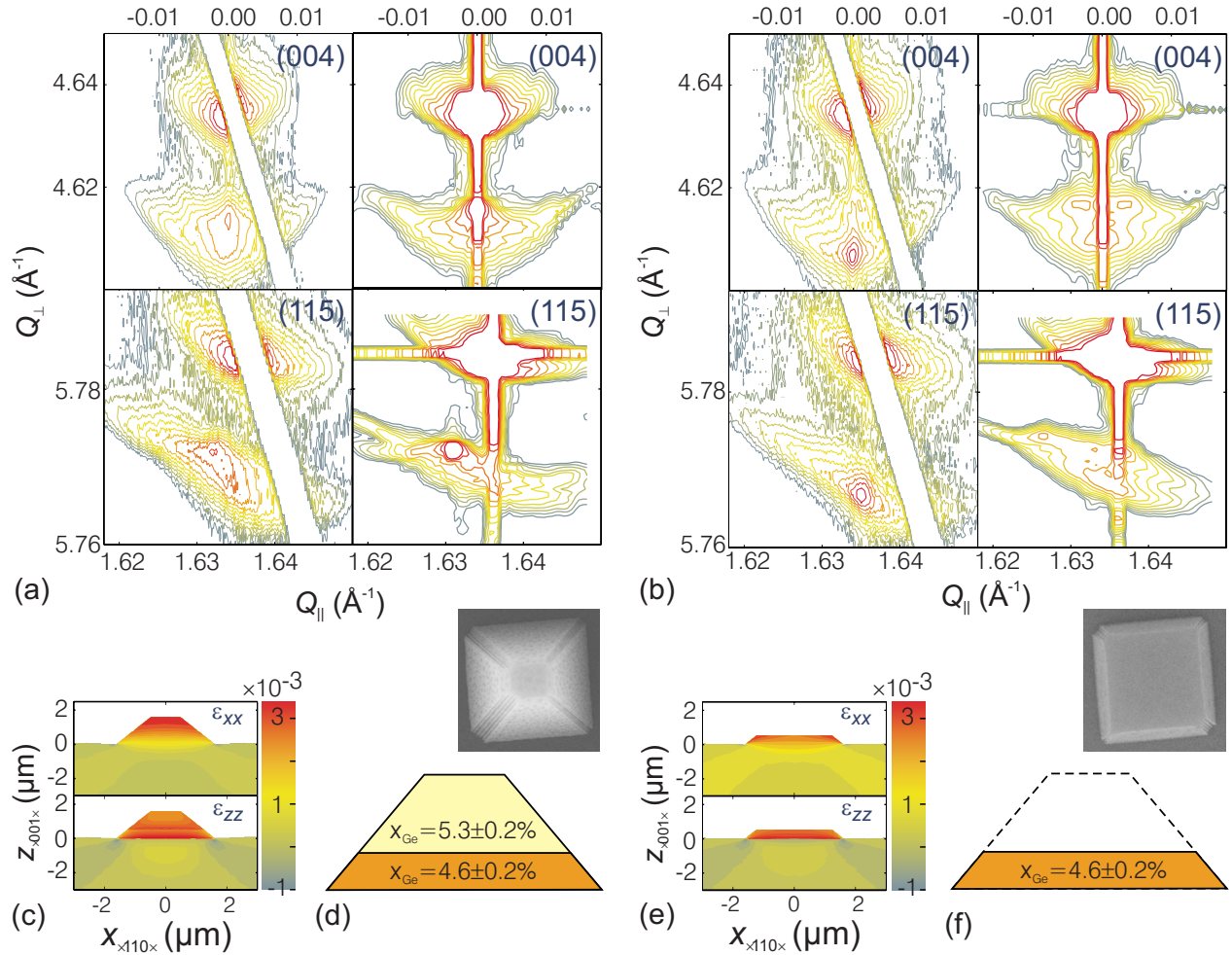
FIG. 3. (Color online) (a), (b) Experimental (left) and simulated (right) intensities for individual truncated and flat islands (SEM in inset). (c), (e) ε_{xx} and ε_{zz} strain tensor components. The top of the truncated pyramids is fully relaxed, whereas the relaxation in the flat ones reaches only about 50%. (d), (f) Ge distribution from the best fit. The flat islands are found to represent the bottom part of the truncated pyramids.

tion of the x-ray data, one can infer that the aspect ratio (height/width) of the latter island is smaller than that of the former: the peak positions in reciprocal space show different relaxation, but almost the same Ge content. Since relaxation depends mainly on Ge content and island shape, less relaxation corresponds to a smaller aspect ratio:[28] efficient relaxation requires that the island top can expand sideways, which is facilitated if the aspect ratio is high.

III. ANALYSIS OF STRAIN AND COMPOSITION

A quantitative analysis is performed by using the island shape of a truncated pyramid, with the dimensions taken from the scanning electron microscopy (SEM) image of the very same island shown in the insets of Figs. 2(d) and 2(f), and assuming a Ge concentration profile along the growth direction. The three-dimensional strain distribution is calculated using a commercial finite element method (FEM) program package,[29] and the pattern of scattered intensities is simulated using semikinematical scattering theory.[3] In our analysis, we did not include lateral variations of the Ge content.[9,30–32] It has been shown[21,24] that lateral composition

gradients are rather negligible in LPE, where growth occurs close to thermodynamic equilibrium, and diffusion processes in the melt are dominant instead of surface diffusion, which prevails in molecular beam epitaxy. In the FEM model, we consider the nonlinear lattice parameter variation with Ge content as obtained in Ref. 33. The elastic constants are interpolated linearly between the values of Si and Ge,[34] taking into account the slight elastic anisotropies. The islands are placed on a square piece of substrate. For the lateral boundaries of the substrate we assumed periodic boundary conditions, while the substrate bottom was completely fixed. The lateral substrate dimensions and its thickness are chosen large enough so that the boundaries have negligible influence on the calculated strain fields.

The Ge concentration profile along the growth direction is adapted to reach a close match between the measurements and the simulations, as shown in Fig. 3. The same model has to match simultaneously the RSMs around (004) and (115) reflections, thus, increasing the sensitivity for details in the Ge concentration profile. Our method not only allows us to determine the strain in single epitaxial structures, as shown in Figs. 3(c) and 3(e), but also, with a high sensitivity ($\pm 0.2\%$), concentration variations in the individual islands.

For the ensemble average and the single island representative for the average island, a Ge content of $4.6 \pm 0.2\%$ for the bottom part and $5.3 \pm 0.2\%$ for the top part [Fig. 3(d)], with a step at 1/3 of the island height, is obtained. Similar results have been obtained also for LPE-grown island ensembles with much higher Ge contents in previous experiments.[6,21,24] In order to explain the different intensity distribution observed in Figs. 2(e) and 2(f), the aspect ratio of the island needs to be lowered. The simulations show that the flat islands actually represent the 1/3 bottom part of the higher islands, with the same Ge content of $4.6 \pm 0.2\%$, indicated in Fig. 3(f).

Close inspection of the sample using SEM reveals that the "flat" island IL2 has about the same base size as the average island IL1, but only about 1/3 of its height. We measured a set of 24 single islands on a $\sim 300 \times 500$ μm^2 area (part of it shown in Fig. 1) and cross-checked the results using SEM and optical microscopy: there are clearly two different types of islands present, with only about 3% of all islands being of the "flat" type. Since the peak intensity of the x-ray diffraction signal scales with the square of the island volume, in a scattering experiment using a wide beam, only 0.8% of the scattered signal is due to the flat islands, which is impossible to isolate from the total signal. In an experiment sensitive to the ensemble, the higher islands always dominate, and the flat islands go unnoticed. Our results support a scenario in which first a flat "island base" grows, while the "top part" of the islands with a different composition forms only in a second growth step. Only with local resolution can the flat islands be characterized in detail, which supplies important information for modeling the growth. A very high resolution in strain and Ge composition is provided by our study. For the low overall Ge content, this accuracy is mandatory to reveal the details in the Ge distribution in the growth direction.

IV. SUMMARY

We have demonstrated the combination of high-resolution XRD with local (lateral) resolution in real space using a microfocused x-ray beam for the detailed characterization of micron-sized single SiGe islands on Si(001). We combined local probe x-ray diffraction with SEM analysis, yielding a complete structural characterization of individual islands (shape, strain, composition). Differences between the morphology, strain, and chemical composition of individual islands (truncated and flat pyramids) are clearly correlated and resolved, with a sensitivity hardly achievable by other techniques. The approach can be applied without modification to the analysis of buried islands and is compatible with anomalous x-ray scattering, offering enhanced chemical sensitivity.

Note added in proof, After the submission of this manuscript we became aware of the paper by M. Hanke *et al.*[35] on scanning x-ray diffraction on single SiGe islands.

[1] P. Offermans, P. M. Koenraad, J. H. Wolter, K. Pierz, M. Roy, and P. A. Maksym, Phys. Rev. B **72**, 165332 (2005).

[2] D. L. Sales, J. Pizarro, P. L. Galindo, R. Garcia, G. Trevisi, P. Frigeri, L. Nasi, S. Franchi, and S. I. Molina, Nanotechnology **18**, 475503 (2007), and references therein.

[3] J. Stangl, V. Holý, and G. Bauer, Rev. Mod. Phys. **76**, 725 (2004).

[4] T. H. Metzger, T. U. Schülli, and M. Schmidbauer, C. R. Phys. **6**, 47 (2005).

[5] I. Kegel, T. H. Metzger, A. Lorke, J. Peisl, J. Stangl, G. Bauer, K. Nordlund, W. V. Schoenfeld, and P. M. Petroff, Phys. Rev. B **63**, 035318 (2001).

[6] Th. Wiebach, M. Schmidbauer, M. Hanke, H. Raidt, R. Köhler, and H. Wawra, Phys. Rev. B **61**, 5571 (2000).

[7] T. U. Schülli, J. Stangl, Z. Zhong, R. T. Lechner, M. Sztucki, T. H. Metzger, and G. Bauer, Phys. Rev. Lett. **90**, 066105 (2003).

[8] A. Malachias, S. Kycia, G. Medeiros-Ribeiro, R. Magalhães-Paniago, T. I. Kamins, and R. S. Williams, Phys. Rev. Lett. **91**, 176101 (2003).

[9] M. S. Leite, G. Medeiros-Ribeiro, T. I. Kamins, and R. S. Williams, Phys. Rev. Lett. **98**, 165901 (2007).

[10] C. G. Schroer and B. Lengeler, Phys. Rev. Lett. **94**, 054802 (2005).

[11] F. Pfeiffer, C. David, M. Burghammer, C. Riekel, and T. Salditt,

[12] A. Jarre, C. Fuhse, C. Ollinger, J. Seeger, R. Tucoulou, and T. Salditt, Phys. Rev. Lett. **94**, 074801 (2005).

[13] B. C. Larson, Wenge Yang, G. E. Ice, J. D. Budai, and J. Z. Tischler, Nature (London) **415**, 887 (2002).

[14] J. D. Budai, Wenge Yang, N. Tamura, J.-S. Chung, J. Z. Tischler, B. C. Larson, G. E. Ice, C. Park, and D. P. Norton, Nat. Mater. **2**, 487 (2003).

[15] C. Riekel, Rep. Prog. Phys. **63**, 233 (2000).

[16] Y. Xiao, Z. Chai, and B. Lai, Nanotechnology **16**, 1754 (2005).

[17] B. Krause, C. Mocuta, T. H. Metzger, C. Deneke, and O. G. Schmidt, Phys. Rev. Lett. **96**, 165502 (2006).

[18] P. Fenter, C. Park, Z. Zhang, and S. Wang, Nat. Phys. **2**, 700 (2006).

[19] J. Miao, C.-C. Chen, C. Song, Y. Nishino, Y. Kohmura, T. Ishikawa, D. Ramunno-Johnson, T.-K. Lee, and S. H. Risbud, Phys. Rev. Lett. **97**, 215503 (2006).

[20] M. A. Pfeifer, G. J. Williams, I. A. Vartanyants, R. Harder, and I. K. Robinson, Nature (London) **63**, 442 (2006).

[21] M. Schmidbauer, *X-Ray Diffuse Scattering from Self-Organized Mesoscopic Semiconductor Structures*, Springer Tracts in Modern Physics Vol. 199 (Springer, Berlin, 2004).

[22] D. J. Jensen, E. M. Lauridsen, L. Margulies, H. F. Poulsen, S. Schmidt, H. O. Sørensen, and G. B. M. Vaughan, Mater. Today

Science **297**, 230 (2002).

9, 18 (2006).

[23] J. M. Yi, J. H. Je, Y. S. Chu, W. G. Cullen, and H. You, Nucl. Instrum. Methods Phys. Res. A **551**, 157 (2005).

[24] M. Hanke, M. Schmidbauer, D. Grigoriev, H. Raidt, P. Schäfer, R. Köhler, A.-K. Gerlitzke, and H. Wawra, Phys. Rev. B **69**, 075317 (2004).

[25] D. Grützmacher, T. Fromherz, C. Dais, J. Stangl, E. Müller, Y. Ekinci, H. H. Solak, H. Sigg, R. T. Lechner, E. Wintersberger, S. Birner, V. Holý, and G. Bauer, Nano Lett. **7**, 3150 (2007).

[26] The minimum achievable focus size is at present 400×1200 nm^2 with a gain of a few 10^4; here we chose a focus size adapted to the size of the investigated islands.

[27] In the Si substrate, the SiGe islands lead to a tensile strain below the center of the islands and to a compressive one below the island circumference. Also these strain differences could be used for imaging, however, due to the comparatively large Si volume contribution to the scattered intensity—the penetration depth in coplanar XRD is in the order of several 10 μm depending on wavelength and incidence and exit angles—diffuse scattering from point defects blurs this intensity contrast in our case.

[28] A. Hesse, J. Stangl, V. Holý, T. Roch, G. Bauer, O. G. Schmidt, U. Denker, and B. Struth, Phys. Rev. B **66**, 085321 (2002).

[29] Comsol Multiphysics with structureal mechanics module, for details see http://www.comsol.com/

[30] G. Katsaros, M. Stoffel, A. Rastelli, O. G. Schmidt, K. Kern, and J. Tersoff, Appl. Phys. Lett. **91**, 013112 (2007).

[31] G. Hadjisavvas and P. C. Kelires, Phys. Rev. B **72**, 075334 (2005).

[32] Y. Tu and J. Tersoff, Phys. Rev. Lett. **98**, 096103 (2007).

[33] D. De Salvador, M. Petrovich, M. Berti, F. Romanato, E. Napolitani, A. Drigo, J. Stangl, S. Zerlauth, M. Mühlberger, F. Schäffler, G. Bauer, and P. C. Kelires, Phys. Rev. B **61**, 13005 (2000).

[34] O. Madelung, *Semiconductors-Basic Data* (Springer, Berlin, 1996).

[35] M. Hanke *et al.*, Appl. Phys. Lett. **92**, 193109 (2008).